Korean J. Chem. Eng., 33(10), 2878-2890 (2016)
DOI: 10.1007/s11814-016-0155-x

pISSN: 0256-1115
eISSN: 1975-7220

Application of mesoporous magnetic carbon composite for reactive dyes removal: Process optimization using response surface methodology

Ahmad Jonidi Jafari*,, Babak Kakavandi***,****,†, Roshanak Rezaei Kalantary*,**, Hamed Gharibi*****, Anvar Asadi******, Ali Azari*******, Ali Akbar Babaei****, and Afshin Takdastan******

*Research Center for Environmental Health Technology (RCEHT), Iran University of Medical Sciences, Tehran, Iran
**Department of Environmental Health Engineering, School of Public Health, Iran University of Medical Sciences, Tehran, Iran
***Student Research Committee, Ahvaz Jundishapur University of Medical Sciences, Ahvaz, Iran
****Department of Environmental Health Engineering, School of Health, Ahvaz Jundishapur University of Medical Sciences, Ahvaz, Iran
*****School of Public Health, Shahroud University of Medical Sciences, Shahroud, Iran
******Department of Environmental Health Engineering, School of Public Health, Shahid Beheshti University of Medical Sciences, Tehran, Iran
*******Department of Environmental Health Engineering, School of Public Health, Tehran University of Medical Sciences, Tehran, Iran
(*Received 17 February 2016 • accepted 8 June 2016*)

Abstract−Discharging the effluents of textile wastewaters into potable water resources can endanger the ecosystem, due to their reactivity, toxicity, and chemical stability. In this research, the application of powder activated carbon modified with magnetite nanoparticles (PAC-MNPs) as an adsorbent for removal of reactive dyes (Reactive black 5 (RB5) and reactive red 120 (RR120)) was studied in a batch system. The adsorption performance was evaluated as a function of temperature, contact time and different adsorbent and adsorbate concentrations. The levels of factors were statistically optimized using Box-Behnken Design (BBD) from the response surface methodology (RSM) to maximize the efficiency of the system. The adsorption process of both dyes was fit with the pseudo-second order kinetic and Langmuir isotherm models. The identified optimum conditions of adsorption were 38.7 °C, 46.3 min, 0.8 g/L and 102 mg/L for temperature, contact time, adsorbent dose, and initial dyes concentration, respectively. According to the Langmuir isotherm, the maximum sorption capacities of 175.4 and 172.4 mg/g were obtained for RB5 and RR120, respectively. Thermodynamics studies indicated that the adsorption process of the reactive dyes was spontaneous, feasible, and endothermic. After five cycles, the adsorption efficiency was around 84 and 83% for RB5 and RR120, respectively. A high value of desorption was achieved, suggesting that the PAC-MNPs have a good potential in regeneration and reusability, and also can be effectively utilized in industrial applications. PAC-MNPs also show a good anti-interference potential for removal of reactive dyes in dye-industry wastewaters.

Keywords: Reactive Dyes, Response Surface Method, Box-Behnken Design, Adsorption, Magnetic Composite

INTRODUCTION

Ever increasing industrial growth has led to an increased amount of pollutants disposal into the environment. The amount of industrial wastewater effluents containing dyes has recently increased, because dyes and their relative compounds are widely used in industrially for various purposes, including in chemical laboratories for analytical purposes and many biological and biomedical laboratories (e.g., biological stains). The presence of dyes in water resources reduces the penetration of light into water, which not only could result in lowering the rate of photosynthesis and oxygen production, but also could endanger aquatic organisms and microorganisms [1,2]. Also, dyes are, in fact, of organic nature which their presence in the wastewater effluents not only increases the chemical oxygen demand (COD), but also decreases the biological degradability of the effluents [1,3]. Considering the negative effects, structure and stability of these compounds, their complete removal from water resources and wastewater effluents is an important environmental priority [4,5].

Several technologies are available for removing dyes from aqueous environments, including ion exchange, coagulation and flocculation, adsorption, advanced oxidation and extraction (AOP), membrane filtration and biological methods [2,6-10]. However, most of these methods have their own drawbacks, like the operational and capital costs which are considered to be the limiting factors in applying most of these methods. In addition, there are specific problems regarding sludge disposal and production of hazardous byproducts [11]. The biological methods are not regarded as effective and

†To whom correspondence should be addressed.
E-mail: kakavandi.b@ajums.ac.ir, kakavandibvch@gmail.com

appropriate; time-consuming fermentation processes required for most of these methods and also inability to remove dyes consistently are the main disadvantages [4].

The adsorption process has been widely applied and proven to be a suitable method for treatment of dyed wastewaters. On one hand, there are specific advantages in using the adsorption process, including simple design, ease and low operational cost, insensitivity towards the toxic compounds and removal efficiency even at very low concentrations of contaminants [12-17]. On the other hand, this process requires filtration and centrifugation, which increases the amount of turbidity in the effluents. To overcome these problems, an appropriate way can be the magnetization of the adsorbents where the adsorbent and adsorbed contaminants can be simply and rapidly separated from the solution by means of an external magnetic field [18-21]. To magnetize the adsorbents, iron oxide nanoparticles (IONs), known as magnetic nanoparticles (MNPs) (e.g., Fe_3O_4, α-Fe_2O_3, γ-Fe_2O_3 and FeO (OH)) need to be incorporated with them [11,22,23]. The combination of MNPs (i.e., Fe_3O_4) with the adsorbent could result in having better kinetics for the adsorption of pollutants and also chemical stability. It is noteworthy that the later one originates from the basic properties of PAC (i.e., its extremely small size and also high surface area-to-volume ratio) [16,24,25]. Recently, various adsorbents including multi-wall carbon nanotube [26,27], activated carbon [4], chitosan [28], graphene [29] have been magnetized and applied for decolorization of wastewater effluents.

However, most of these adsorbents suffer from low surface area and adsorption capacity, complex synthesis procedure, high cost of raw materials and difficult accessibility. In contrast, PAC provides a noticeable adsorption capacity for contaminants removal and exhibits high potential as a supporting for uniform distribution of MNPs, due to high specific surface area, porosity and easy availability. Therefore, in the present study, a composite of PAC and magnetite nanoparticles (PAC-MNPs) was prepared, characterized and then used as an adsorbent for removal of reactive dyes (Reactive Black 5 (RB5) and Reactive Red 120 (RR120)) from aqueous solutions. Herein, magnetic composite was synthesized with two goals: (i) to use PAC-MNPs with a high adsorption capacity as a first study on adsorption of RB5 and RR120 from aqueous solution, and (ii) to solve the operational problems of PAC such as filtration, centrifugation, and causing turbidity in the effluents. To describe the experimental data, the kinetics, equilibrium isotherms and thermodynamics of the adsorption of dyes were fully studied. The experiments were designed and optimized by using response surface methodology (RSM) approach.

MATERIALS AND METHODS

1. Reagents and Equipment

All chemicals were of analytical-laboratory grade and purchased from Sigma (Sigma-Aldrich., Germany) and used without further purification. Two commercial textile dyes, Reactive Black 5 (RB5, 55% purity) and Reactive Red 120 (RR120, ≥50% purity), were used to prepare the stock solution. The structure and specific physicochemical properties of the investigated dyes are given in Supplementary data Table S1. Ferrous sulfate heptahydrate ($FeSO_4 \cdot 7H_2O$ ≥99.5%), powder activated carbon (PAC) and NaOH were applied to prepare the adsorbent. Deionized water (DI-water) was also used throughout all the experiments for preparation of required solutions. In addition, 0.1 M hydrochloric acid (0.1 M HCl) solution was used to adjust the pH of solutions. The concentration of the residual dyes in the solution was measured using a UV-Visible spectrophotometer (DR 5000, HACH Co., USA) at their maximum absorption wavelength. To evaluate the stability of PAC-MNPs, the concentration of total iron leached from the adsorbent into the solution was measured by atomic absorption spectrophotometry (AAS, Shimadzu AA 6800) with respect to the ASTM D1068-90 method [30].

2. Adsorbent Synthesis

The composite of PAC-MNPs with small alerts was prepared in accordance to co-precipitation technique given in our previous work [20]. In brief, by adding 0.556 g of $FeSO_4$ into 200 mL of DI-water under nitrogen atmosphere, 10 mmol ferrous sulfate solution was prepared and then 1 g of PAC was added into the solution. The obtained suspension was mixed using a magnetic stirrer, while 20 mL of 10% NaOH solution was added dropwise into the suspension for 5 min to precipitate the hydrated iron oxides. During the addition of NaOH solution, the color of the suspension became dark brown at pH~6 and then turned to black at pH~10. The suspension was then vigorously stirred for 1 h at 100 °C. At this stage, the suspension was cooled at room temperature, then the resultant magnetic adsorbent was separated employing an external magnetic field and washed several times with DI-water until its pH reached neutral state. All non-magnetic PAC particles were removed from the sample during the washing cycles. After washing, the as-synthesized composite was dried at 105 °C in an oven for 1 h, and finally stored in an air-tight container to be used for the future experiments.

3. Characterization of the Adsorbent

In the present study, a transmission electron microscope (TEM, PHILIPS, EM) at 100 kV was used to characterize the shape and size of synthesized MNPs. The surface morphology of PAC-MNPs and the magnetite distribution within the PAC were analyzed using a scanning electron microscope (SEM, PHILIPS, XL-30) at 25 kV. The sample was set in epoxy and then placed in the sample chamber and evacuated by using high vacuum (5×10^{-7} Torr). The sample was bombarded with a finely focused electron beam. A three-dimensional topographic image (SEM micrograph) was formed by collecting the secondary electrons generated by the primary beam. An energy dispersive X-ray (EDX, PHILIPS, XL-30) technique was also used to characterize the elemental composition of the adsorbent. This technique was carried out on sintered pellets by a Zeiss EVO 40 scanning electron microscope in conjunction with EDX system. The XRD pattern of PAC, MNPs and PAC-MNPs were analyzed (Quantachrome, NOVA 2000) using graphite monochromatic copper radiation (Cu Kα, λ=1.54 Å) at 25 °C. Samples were placed in a zero background metal holder and scanned from 2θ of 5° to 70° with a scanning speed of 2° 2θ min^{-1}. BET analysis (Quantachrome, 2000, NOVA) was applied to determine the surface area of the synthesized adsorbent. Prior to the measurement, the sample was degassed at 100 °A for 8 h in an out-gassing station to remove any adsorbed water or entrapped gases. Magnetic properties of

PAC-MNPs were investigated by a vibrating sample magnetometer (VSM) (7400, Lakeshore, USA) at room temperature.

4. Adsorption Study

The stock solution of dyes (500 mg/L) was prepared by dissolving an accurately weighed amount of RB5 and RR120 in DI-water. The adsorption experiments of RB5 and RR120 dyes onto PAC-MNPs were conducted in a batch environment in 100 mL conical flasks containing 50 mL of the prepared solutions of dyes. All conical flasks were sealed to remove the effect of irradiation on the adsorption process performance. In this study, the effect of different experimental variables including contact time, different adsorbent and adsorbate concentrations and solution temperature on the removal efficiency of dyes was investigated. All the experiments were at an optimum pH of 4±0.5, which was obtained through pre-experiments. First, the samples were shaken at a constant rate of 200 rpm to reach adsorption equilibrium conditions. At appropriate time intervals, the aliquots were withdrawn from the solutions and the adsorbent was separated by using a magnet. The remaining concentrations of dyes were measured using a UV-Visible spectrophotometer at the respective λ_{max} values (597 nm for RB5 and 511 nm for RR120). All the experiments, except for the BBD method, were in triplicate, and the mean and the standard deviation (SD) of the values were used to calculate the final results. The adsorption capacity (q_e) and the removal efficiency (R%) of RB5 and RR120 dyes were obtained through the following equations:

$$\text{Dye adsorption capacity (mg/g)} = (C_0 - C_e)\left(\frac{V}{m}\right) \quad (1)$$

$$\text{Dye removal efficiency (\%)} = 100 \times \left(1 - \frac{C_e}{C_0}\right) \quad (2)$$

where, C_0 and C_e are the initial and equilibrium dyes concentrations (mg/L), respectively. V, m, and q_e are the volume of the solution (L), the dry weight of the adsorbent (g), and the amount of adsorption capacity at equilibrium time (mg/g), respectively.

5. Experimental Design

Response surface methodology (RSM) is a combination of statistical and mathematical methods used to distinguish the best conditions for conducting the experiments with the least number of required experiments. In addition, it was applied as an empirical study for examining the relationship between the measured responses and the number of independent variables with the purpose of optimizing the response. A three-level factorial design was established using Design Expert software 8.0 (Stat-Ease Inc., Minneapolis MN, USA) following Box-Behnken methodology. Box-Behnken design (BBD) was used to clarify the relationship between the independent variables and the response function.

In this work, four independent variables were designated including, X_1 (temperature, °C), X_2 (contact time, min), X_3 (dose of PAC-MNPs, g/L), and X_4 (initial dye concentration, mg/L). In addition, the low (−1), middle (0) and high (+1) levels of each variable were designated. The experimental ranges and levels of the mentioned independent variables are shown in Table 1. Removal percentage of dyes (Y) was regarded as the response of the system. To compare different variables with various units, the actual values of the variables (denoted as X_i) were coded based on the following equation:

Table 1. Independent variables and response of adsorption

Independent variables	Symbols	Ranges and levels		
		−1	0	+1
Temperature (°C)	X_1	25	35	45
Contact time (min)	X_2	20	40	60
Adsorbent dose (g/L)	X_3	0.5	1	1.5
Initial dye concentration (mg/L)	X_4	50	100	150

$$A_i = \frac{X_i - X_0}{\Delta x} \quad (3)$$

where, A_i is the coded value of the variable, Δx is the difference between the high and the median values of the variable and X_0 refers to the median value of the variable.

A total of 29 experiments was set upon, for which the coefficients of the second-order polynomial regression model for four variables with three levels were calculated. The behavior of the adsorption process can be explained based on the following empirical second-order polynomial model Eq. (4):

$$Y = b_0 + \sum_{i=1}^{n} b_i x_i + \sum_{i=1}^{n} b_{ii} x_i^2 + \sum_{i=1}^{n-1} \sum_{j=i+1}^{n} b_{ij} x_i x_j \quad (4)$$

where, Y is the predicted response (dye removal efficiency), b_0 is a constant while, b_i, b_{ii} and b_{ij} stand for the linear coefficient, quadratic coefficient and interaction effect coefficient, respectively. x_i and x_j are also the coded values of the variables. In addition, analysis of variance (ANOVA) was used to analyze the results and also to check the statistical significance of the fitted quadratic models. The optimal values of the critical parameters for adsorption process were calculated by using the fitted models and then validated based on the results of the experiments.

6. Elution and Regeneration Experiments

The regeneration of the adsorbent should be taken into account when one wants to lower the cost of the adsorption process and also recover the pollutants extracted from wastewater. Since the adsorption of RB5 and RR120 dyes on the PAC-MNPs is a reversible process, there is a possibility in either regenerating or activating the adsorbent in terms of reusability. In the present study, first, the performance of dyes adsorption with an initial concentration of 50 mg/L for five consecutive adsorption-desorption cycles was assessed under the following conditions: 60 min contact time and adsorbent dose of 1 g/L. At the end of each adsorption cycle, desorption experiments were carried out using 0.1 M NaOH solution as a desorbing agent. Based on the reports of researchers who previously employed NaOH as a desorbing agent to desorb contaminants from different loaded adsorbents magnetized by Fe_3O_4 NPs, this agent has a high desorption ability [31,32]. In addition, it was selected to avoid damaging the adsorbent and/or physical changes in its structure. Here, 0.1 g of PAC-MNPs loaded with RB5 and RR120 dyes was added to 10 mL of 0.1 M NaOH solution and then placed on a shaker for 12 h at 200 rpm and 25±1 °C.

The regeneration efficiency (%RE) of composite was calculated using Eq. (5). The adsorbent was thereafter repeatedly washed with DI-water and finally dried in an oven at 100 °C for 6 h and then reused for the subsequent adsorption-desorption cycle.

$$(\%RE)=\left(\frac{q_r}{q_0}\right)\times 100 \quad (5)$$

where q_o and q_r (mg/g) are respectively the adsorption capacities of PAC-MNPs before and after regeneration.

RESULTS AND DISCUSSION

1. Properties of Adsorbent

Fig. 1(a) and (b) show the TEM image of MNPs at 25 keV and the SEM image of PAC-MNPs at 100 keV, respectively. The TEM micrograph of MNPs reveals spherical structure of magnetic particles with the average diameter of 30-80 nm. It can be seen that the color of the center of the sphere is darker than the other parts, confirming the presence of MNPs. However, due to the coating of carbon, the color of the edge of the sphere is lighter than the other parts. In addition, the SEM image shows uniform distribution of the pores on the PAC, suggesting the good porosity of the synthesized adsorbent. It also depicts that the external surface of the adsorbent is rough and has some cavities. The elemental analysis of PAC-MNPs, which was conducted using EDX (Fig. 1(c)), confirms the presence of specific elements including carbon, oxygen, iron, lead and zinc in the structure of the adsorbent. It also illustrates that the PAC-MNPs structure consists of 71.6% carbon, 8.3% oxygen and 20.1% iron. From EDX results, it can be implied that iron and oxygen were the major elements of the coating. The presence of trace amounts of lead and zinc represents that there are very minor impurities in the structure of PAC.

Furtheremore, XRD analysis was conducted by using Cu Kα radiation at 25 °C. The results shown in Fig 1(d) indicate a broad peak (2θ=22°) observed in the pattern of PAC. In other words, it reflects the characteristics of carbon amorphous nature. Note that the XRD pattern of MNPs was consistent with the PDF card in the database (Joint Committee for Power Diffraction Studies, Card No. 19-0629). Six narrow peaks at 2θ of 30.07°, 35.44°, 43.15°, 54.6°, 56.99° and 62.6° were in correspondance to the (220), (311), (400), (422), (511), and (440) plane of the orthorhombic magnetite, respectively. These peaks as well as the peak assigned to carbon (2θ=25°) were also observed in the pattern of synthesized PAC-MNPs composite, indicating successful synthesis of magne-

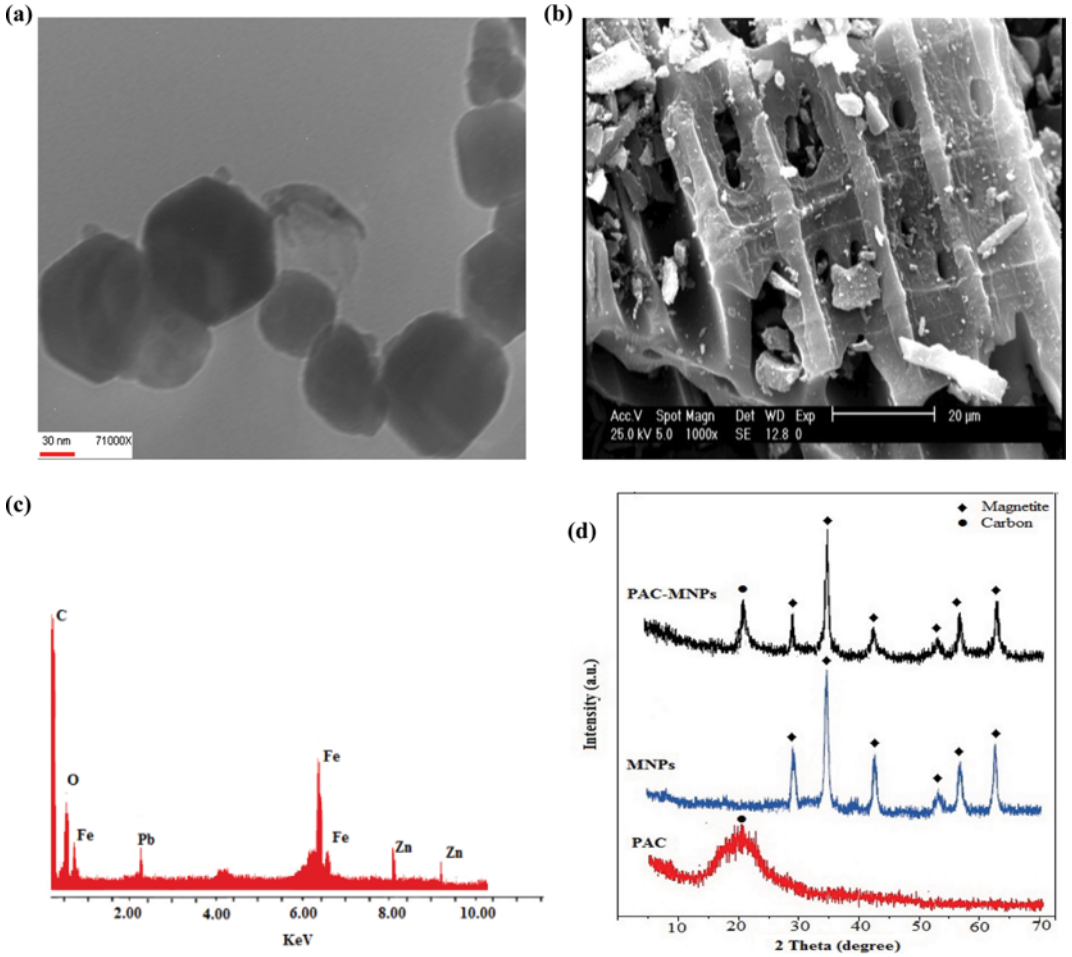

Fig. 1. Characterization of PAC-MNPs: (a) TEM photograph of MNPs; (b) SEM photograph of PAC-MNPs; (c) EDX spectrum of PAC-MNPs and (d) XRD pattern of PAC, MNPs and PAC-MNPs.

Table 2. Main characteristics of adsorbents synthesized in this study

Parameter	Unit	Value		
		PAC	MNPs	PAC-MNPs
Specific surface area (BET)	m^2/g	936	66.3	728.7
Pore volume	cm^3/g	0.753	0.008	0.436
Average pore diameter	nm	5.24	0.85	3.7
Pore structure	-	Mesopore	Micropore	Mesopore
pH_{ZPC}	-	7.9±0.2	-	6.4±0.2
Color	-	Black	Black	Black

tite crystals on the carbon surfaces. The existence of MNPs in the composite structure confirms that the obtained adsorbent can be separated from aqueous solutions using magnets. These results show that the nature of both MNPs and PAC-MNPs composite was crystalline. Although the carbon is amorphous, the observed crystallinity of the PAC-MNPs can be derived from the presence of iron oxide [33].

The specific surface area, volume and average pore diameter of MNPs, PAC and PAC-MNPs were measured using the BET methods and the relative results are shown in Table 2. As can be seen from the table, the average pore size was 3.7 nm. On the basis of IUPAC classification (micropores (d<2 nm), mesopores (2<d<50 nm) and macropores (d>50 nm)), this could be classified into the mesopores groups [34]. The total pore volume obtained at p/p_0= 0.99 by BET was 0.436 cm^3/g. Results of the BET analysis also indicated that the highest surface area of PAC-MNPs was 728.7 m^2/g, which is slightly less than that of PAC (936 m^2/g). Note that the reason for this observation could be due to the filling of pores on PAC by MNPs. Fig. 2 shows the VSM magnetization curve of MNPs and PAC-MNPs at 25 °C in the cycling magnetic field of −10 kOe to +10 kOe. Maximum saturation of magnetization for MNPs and PAC-MNPs was, respectively, about 8.6 and 6.2 emu/g. The magnetization value for PAC-MNPs composite was less than its corresponding amount for the naked MNPs. In fact, this could be due to the presence of non-magnetic PAC in the composite structure. This saturation of magnetization (6.2 emu/g) was higher than that

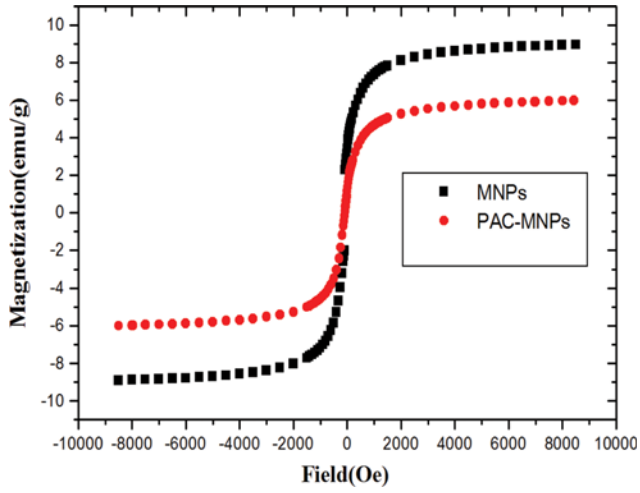

Fig. 2. Magnetization curves of MNPs and PAC-MNPs.

reported in previously conducted studies as a sufficient magnetization amount for magnetic separation of adsorbents [35,36]. This finding demonstrates that the PAC-MNPs exhibit an excellent magnetic response to a magnetic field. Therefore, this magnetic composite could be employed as an adsorbent for environmental purposes. Additionally, this adsorbent can easily and rapidly be removed from the solution without generating secondary pollution.

2. Experimental Design and Development of Regression Model

The full factorial BBD with four factors at three levels, the maximum observed and predicted response and the residuals are listed in Table 3. A total of 29 batch runs based on the BBD-designed experiments with five replicates at central point was investigated to evaluate the effects of the independent factors on the response. Based on the obtained results, the removal efficiencies of the RB5 and RR120 varied between 55.3-99.4% and 53-94.5%, respectively. The highest removal efficiencies of RB5 and RR120 were 99.38 and 94.5%, respectively, obtained during the sixth run of the experiment with the maximum operational conditions of 1.5 g/L adsorbent, 40 min contact time, 50 mg/L initial dye concentration and 35 °C temperature. According to the RSM results, the second-order polynomial equation, as shown below, was obtained for each dye:

$$\begin{aligned}\text{Removal (RB5)} = {} & +61.50603+(1.48671X_1)+(0.25025X_2)\\ & +(24.43207X_3)-(0.28077X_4)+(0.015907X_1X_2)\\ & +(0.38122X_1X_3)+(6.51000E\text{-}003X_1X_4)\\ & +(+0.21072X_2X_3)+(1.61750E\text{-}003X_2X_4)\\ & +(+0.15410X_3X_4)-(0.040613X_1^2)\\ & -(0.012326X_2^2)-(24.02769X_3^2)-(2.24725E\text{-}003X_4^2)\end{aligned} \quad (6)$$

$$\begin{aligned}\text{Removal (RR120)} = {} & +30.48458+(+1.85750X_1)+(1.01444X_2)\\ & +(22.80489X_3)-(0.11666X_4)\\ & +(4.40646E\text{-}003X_1X_2)+(0.10517X_1X_3)\\ & +(4.85000E\text{-}003X_1X_4)+(0.020967X_2X_3)\\ & -(8.87500E\text{-}004X_2X_4)+(0.12550X_3X_4)\\ & -(0.034532X_1^2)-(0.012521X_2^2)\\ & -(13.51381X_3^2)-(2.19744E\text{-}003X_4^2)\end{aligned} \quad (7)$$

Eqs. (6) and (7) show how the particular factor and the interaction between the two factors affect the sorption of dyes by PAC-MNPs. The negative and positive coefficients in the above-mentioned equations described negatively and positively the effect on the dyes removal. A positive impact of a factor means an improvement in the response when the factor level increases, while a negative impact means that the response is not improved with increasing the factor levels. According to Eqs. (6) and (7), the factors X_1, X_2, and X_3

Table 3. Experimental design based on Box-Behnken design (BBD) used in this study

Run no.	Independent factors				Observed (R%)		Predicted (R%)		Residual	
	X_1	X_2	X_3	X_4	RB5	RR120	RB5	RR120	RB5	RR120
1	25	20	1	100	79.19	73.54	79.84	74.42	−0.65	−0.88
2	45	20	1	100	79.32	75.48	79.72	76.79	−0.4	−1.31
3	25	60	1	100	81.54	76.6	81.21	76.63	0.33	−0.028
4	45	60	1	100	94.2	85.4	93.82	82.52	0.38	2.88
5	35	40	0.5	50	92.47	86.73	92.27	88.72	0.2	−1.99
6	35	40	1.5	50	99.38	94.52	98.12	95.29	1.26	−0.77
7	35	40	0.5	150	55.3	53	56.20	52.80	−0.9	0.2
8	35	40	1.5	150	77.62	73.34	77.47	71.92	0.15	1.42
9	25	40	1	50	96.8	92.68	97.27	92.28	−0.47	0.4
10	45	40	1	50	97.21	93.71	97.01	91.57	0.2	2.14
11	25	40	1	150	62.25	57.87	62.40	57.79	−0.15	0.075
12	45	40	1	150	75.68	68.6	75.16	66.78	0.52	1.82
13	35	20	0.5	100	74.26	71.33	73.16	69.47	1.1	1.86
14	35	60	0.5	100	77.26	74.34	76.68	73.02	0.58	1.32
15	35	40	1.5	100	91.5	89.34	93.41	89.10	−1.91	0.24
16	35	60	1.5	100	93.74	89.08	94.46	86.28	−0.72	2.8
17	25	40	0.5	100	74.5	72.05	74.58	71.26	−0.075	0.79
18	45	40	0.5	100	76.11	72.15	77.01	74.34	−0.9	−2.19
19	25	40	1.5	100	85.34	82.7	84.32	83.05	1.02	−0.35
20	45	60	1.5	100	98.8	82.97	98.60	86.30	0.2	−3.33
21	35	20	1	50	93.6	88.6	94.02	87.50	−0.42	1.1
22	35	60	1	50	97.74	92.36	98.52	93.24	−0.78	−0.88
23	35	20	1	150	62.8	58.87	62.43	59.64	0.37	−0.77
24	35	60	1	150	73.41	59.08	73.40	61.83	0.013	−2.75
25	35	40	1	100	92.7	84.28	92.64	86.05	0.061	−1.77
26	35	40	1	100	93.1	85.24	92.64	86.05	0.46	−0.81
27	35	40	1	100	92.38	85.05	92.64	86.05	−0.26	−1
28	35	40	1	100	92.4	86.49	92.64	86.05	−0.24	0.44
29	35	40	1	100	93.67	87.42	92.64	86.05	1.03	1.37

have positive effect on the sorption process of both dyes, while factor X_4 has a negative effect. Therefore, increasing the temperature, contact time and also the adsorbent dosage results in an increase in the adsorption efficiency. The results also indicated that the highest coefficient relates to X_3 (adsorbent dosage) which confirms that this parameter has the highest effect on the dyes adsorption process, compared to the other independent factors.

3. Model Validation

The significance and adequacy of the data of the adsorption process were tested by the ANOVA. In this work, the BBD experimental data were analyzed in two different ways: the sequential model sum of squares and model summary statistics. In fact, these two tests were conducted to obtain regression models and decide about the adequacy of various models (e.g., linear, interactive, quadratic and cubic) so as to represent the adsorption process effectively. Results indicated that the quadratic model quite matched with the experimental data. In other words, it showed higher R^2, adjusted-R^2, predicted-R^2 and also lower p-values for both dyes, in comparison with the other models. The analysis of variance of regression parameters of the predicted response surface quadratic models for reactive dyes removal efficiency and the related results are shown in Supplementary data Table S2.

The values of determination coefficient (R^2) indicated that over 98% of the total variability can be explained by the quadratic model, while only less than 2% of the total variations of both dyes cannot be described by using this model. Moreover, the adjusted regression values of >0.99 and >0.96 were obtained for RB5 and RR120 dyes, respectively, ensuring very good correlations between the model predicted values and the actual experimental ones [20]. The values of adjusted-R^2 also confirmed the high significance of the quadratic model for the adsorption process of the metal ions. Predicted-R^2 describes the prediction capability of the model for new responses; hence, both R^2 and predicted-R^2 should be in a close agreement with each other. As shown in Table S2, R^2, adjusted-R^2 and predicted-R^2 do not differ significantly from each other for both dyes studied in this work [37]. Note that a p-value<0.05 implies that the model terms are significant at confidence level of 95% or more, while the values greater than 0.10 indicate that the model terms are insignificant. As shown in Table S2, a p-value of smaller than 0.0001 was obtained for both dyes, based on the response surface

quadratic model. This suggests that the model is significant and can appropriately explain the relationship between response and independent variables [12].

The lack of fit (LOF), known as F-test, describes the variation of the data around the fitted model. As shown in Table S2, the lack of fit F-values of 0.087 and 0.089 were statistically insignificant for RB 5 and RR120 dyes removal, respectively. An insignificant lack of fit means that there is a significant model in terms of correlation between the variables and dyes removal [38]. The "Adequate Precision" ratio of the model was found to be 59.42 and 26.02 for RB5 and RR120 removal, respectively. Ratios greater than 4 indicate that there is an adequate signal for the model [12]. The coefficient of variance (CV) defines reproducibility of the model and is the ratio of the standard error of estimate to the mean value of the observed responses. Lower CV values of the models clearly indicated that the deviations between experimental and predicted values were low. Relatively low values of CV of the model for RB5 and RR120 dyes removal were 1.17 and 2.87% (<10%), respectively, indicating the precision and reliability of the experiments [20]. The results of ANOVA also showed that the adsorbent dosage was the significant influential experimental variable on the removal of both dyes. The other factors, such as temperature, contact time and initial concentration of dyes, had a comparatively less significant effect on the response.

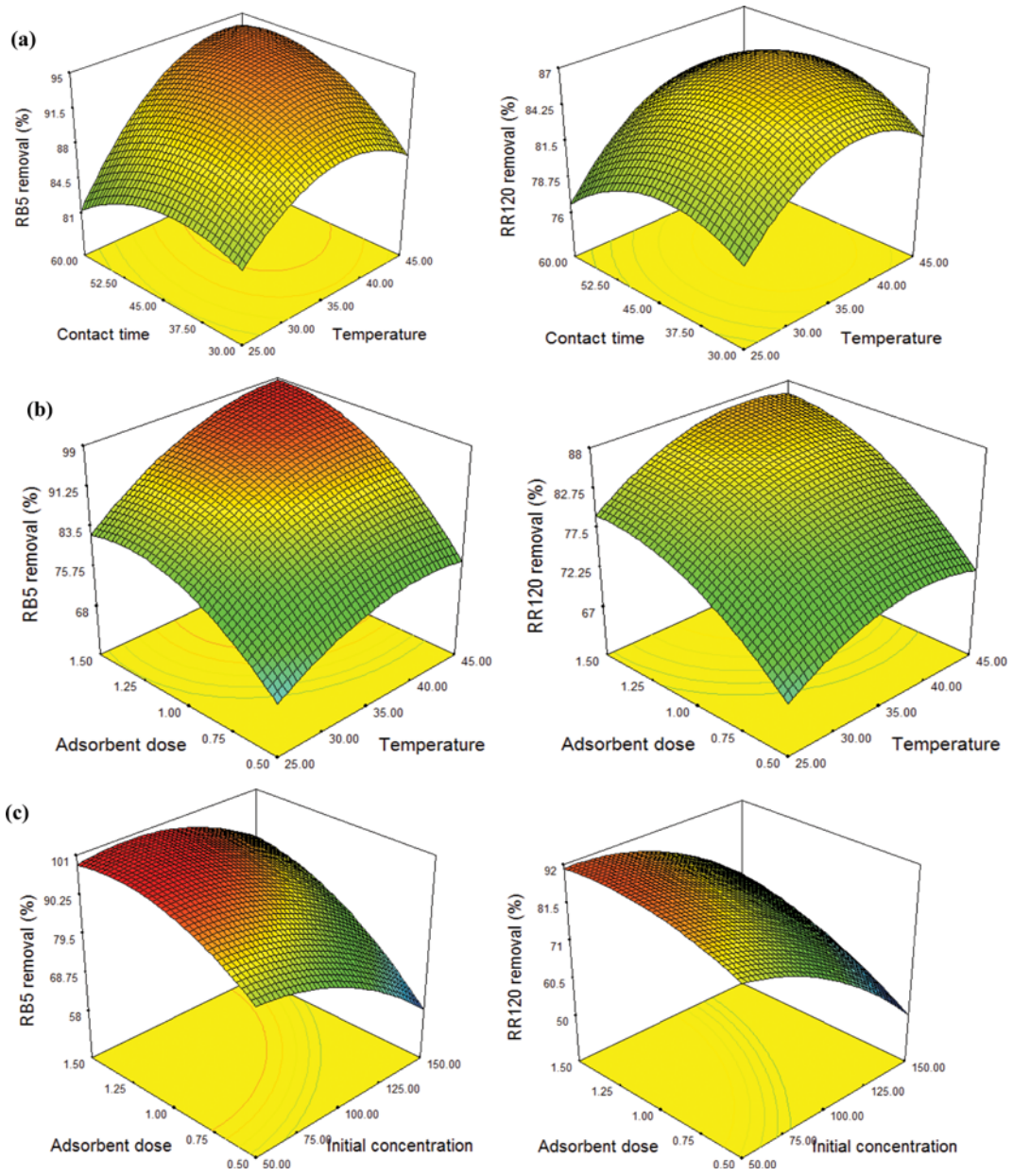

Fig. 3. Response surface plots (3D) showing the variation in RB5 and RR120 dyes removal efficiency as a function of (a) temperature and contact time (1 g/L of adsorbent and 100 mg/L of dye); (b) temperature and adsorbent dose (contact time of 60 min and 100 mg/L of dye); (c) adsorbent dose and initial concentration (contact time of 60 min and 45 °C).

The suitability of developed mathematical models was assessed by constructing diagnostic plots; in other words, we tested predicted outcome versus actual and normal probability plot of the studentized residuals. Fig. S1 shows the relationship between observed and the predicted values for the adsorption process of RB5 and RR120 dyes on PAC-MNPs. The experimental data are the original measure regarding the concentrations of dyes in solution that were calculated using Eq. (2). On the other hand, the predicted values were obtained using statistical model according to Eqs. (6) and (7). Fig. S1(a) and (b) depicts a good correlation between the data obtained by experiments and the predicted values by the model for both dyes. Normal probability plot is also a suitable graphical method for assessing the normality of the residuals. Fig. S2 shows normal probability plot of the studentized residuals for the dye adsorption process. It can be concluded that the residual behavior follows a normal distribution and is linear. This assumption is of high importance for checking statistical modeling. It suggests that the model sufficiently represents the removal of RB5 and RR120 dyes by adsorption process.

4. Main and Interaction Effects

Three-dimensional (3D) response surface plots were depicted to evaluate the effects of the four abovementioned parameters on the removal efficiency of the adsorption process. The interactive effect of contact time and temperature on the removal efficiency of a process in which 1 g/L adsorbent dose and 100 mg/L initial dye concentration were applied as shown in Fig. 3(a). The maximum removal of RB5 and RR120 was achieved when both the temperature and the contact time were high. Considering the direct relationship between removal efficiency and the contact time, the active sites are initially vacant, and increasing the contact time causes the sites to be filled with adsorbate and finally saturated on the surfaces of the adsorbent. Thus, the rapid enhancement of the sorption at initial time is due to the abundance of vacant sites on the adsorbent surface, which enhanced the ability of adsorbing the pollutants. When the adsorbent is saturated with the molecules of the adsorbate, the removal efficiency starts increasing slowly with time [39]. Generally, raising the temperature leads to an enhancement in the uptake of the pollutants through the following ways: i) increasing the mobility of the dye molecules followed by an increase in the effective interactions between the reacting agents and the adsorbent material, and ii) increasing the pore size of the adsorbent surface [40]. Similar observations were also reported in previously conducted studies on organic dyes removal by various types of magnetic composites [4,41].

Fig. 3(b) shows the response surface plots of the interactive influence of adsorbent dose and temperature on dyes removal efficiency when the initial concentration of dyes and contact time were set at 100 mg/L and 60 min, respectively. Under these conditions and also with increasing the adsorbent dose from 0.5 to 1.5 g/L, RB5 and RR120 removal efficiency increased significantly from 77.2 and 72.3% to 98.8 and 97.2%, respectively. A maximum removal for both dyes was observed at temperature of 45 °C and PAC-MNPs dose of 1.5 g/L. Based on the obtained results, we found that with increasing the dosage of PAC-MNPs from 0.5 to 1.5 g/L, the removal efficiency increased. The enhancement in the adsorption can be attributed to the increase in the adsorption surface, and consequently the broad access of the dyes molecules to the adsorption sites on the adsorbent [42,43]. This result is in line with the reports of previous studies regarding the adsorption of dyes on various adsorbents [9,44].

The combined effect of the initial dyes concentration and adsorbent dose (Fig. 3(c)) were assessed under the conditions of 60 min contact time and 45 °C temperature. As shown in Fig. 3(c), more than 98% and 90% of RB5 and RR120 were removed under the mentioned conditions, respectively. Based on the results, the maximum removal percentage of dyes achieved in the present study was related to high adsorbent dosage (1.5 g/L) with minimum dye concentration (50 mg/L). As can be seen from Fig. 3(c), the dye uptake decreased with increasing initial concentration. This could probably be due to the fixed number of active sites on the adsorbent versus an increase in the number of molecules of the dye. Other researchers [1,45] reported that the adsorption efficiency of reactive dyes on the adsorbents dropped significantly when the initial concentration increased.

5. Process Optimization

The main purpose of the optimization is to determine the optimum values of the variables for the removal of reactive dyes by PAC-MNPs from the obtained model and the experimental data. A multiple-response method was used to optimize the removal efficiency of RB5 and RR120, which was a RSM-based strategy. In this regard, the desirability function approach was employed to optimize the different combinations of the selected process parameters. Design Expert software (Version 8.0) provides five options, generally called as none, maximum, minimum, target and within range, which can be applied to choose the desired goal for each variable and response [12]. The purpose of the optimization process is to improve adsorption conditions in a batch process. Therefore, to achieve optimal conditions for removing both dyes using PAC-MNPs, temperature and contact time were set within the range; whereas, the adsorbent dose and initial concentration of dyes were

Table 4. Validation of optimized conditions for RB5 and RR120 dyes adsorption on the PAC-MNPs

Variables	Optimum value	Responses				Desirability
		Observed		Predicted		
		RB5	RR120	RB5	RR120	
Temperature (°C)	38.7	89.42	82.62	91.75	87.92	0.671
Contact time (min)	46.3					
Adsorbent dose (g/L)	0.80					
Initial concentration (mg/L)	102					

set at minimum and maximize levels, respectively. The lower and upper limit values of all responses were deduced from the experimental data of BBD.

The optimum values of the process parameters for the maximum removal efficiency are presented in Table 4. According to the results of BBD, the best local maximum removal for both dyes (91.75% for RB5 and 87.92% for RR120) were obtained at 38.7 °C, contact time of 46.3 min, adsorbent dose of 0.8 g/L and initial concentration of 102 mg/L; besides, the desirability in this case was 0.671. Under these conditions, the removal efficiencies of RB5 and RR120 dyes were 89.42 and 82.62%, respectively. As shown in Table 4, the removal efficiencies for all of the response parameter values, which were either obtained from experiments or estimated from the models, are in a close agreement, confirming the accuracy and validity of the model approach. These results confirmed that the RSM is a powerful tool for optimizing the operational conditions of RB5 and RR120 dyes adsorption onto the PAC-MNPs.

6. Modeling of Adsorption Kinetics, Isotherms, and Thermodynamics

To investigate the mechanism of the adsorption of reactive dyes on the PAC-MNPs and also to find the best fitted model for the experimental data, three kinetic models, pseudo-first-order, pseudo-second-order and intra-particle diffusion models, were considered. The equations and parameters related to these kinetic models are presented in Table 5. Regarding the abbreviations and terms shown in Table 5, q_t (mg/g) is the amount of adsorption capacity at a given time t, and k_1 and k_2 stand for the rate constant of pseudo-first-order and pseudo-second-order sorption, respectively. In addition, k_i (mg/g $min^{0.5}$) represents intra-particle diffusion constant and C_i (mg/g) is a constant value depicting the effects of boundary layer. If the

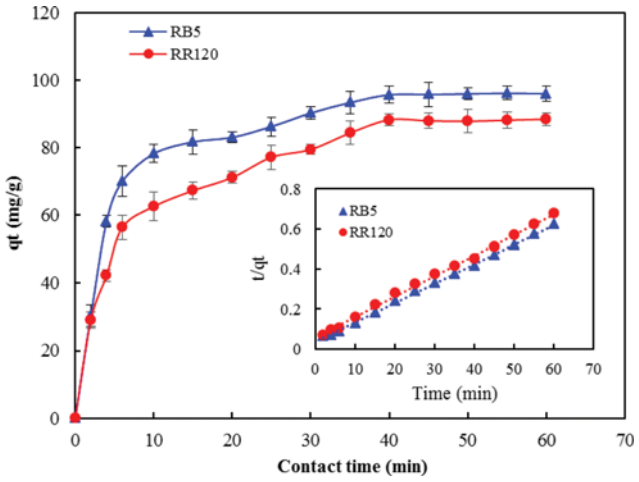

Fig. 4. The effect of contact time on the adsorption capacity of RB5 an RR120 on PAC-MNPs and plots of pseudo-second-order kinetic model of the adsorption process (insert) (experimental conditions: C_0=100 mg/L, adsorbent dose=1 g/L, pH 4±0.5 and 25±1 °C).

Table 5. Values of kinetic and isotherm parameters for sorption of RB 5 and RR 120 on the PAC-MNPs

Models	Linear equations	plot	Dye	Parameters		
Kinetic						
Pseudo-first-order	$Ln(q_e-q_t)=lnq_e-k_1t$	$ln(q_e-q_t)$ vs. t		$q_{e,cal}$ (mg/g)	k_1 (min^{-1})	r^2
			RB5	62.44	0.088	0.9315
			RR120	73.49	0.1	0.9092
Pseudo-second-order	$t/q_t=t/q_e+1/k_2\ q_e^2$	t/q_t vs. t		$q_{e,cal}$ (mg/g)	k_2 (g/mg min)	r^2
			RB5	103.1	0.002	0.9988
			RR120	95.23	0.0018	0.9976
Intra-particle diffusion	$q_t=k_it^{1/2}+C_i$	q_t vs. $t^{0.5}$		k_i (mg/gmin$^{0.5}$)	C_i (mg/g)	r^2
			RB5	10.46	28.6	0.7981
			RR120	10.33	19.85	0.8921
				$q_{e,exp}$ (mg/g)		
			RB5	95.72		
			RR120	85.3		
Isotherm						
Freundlich	$lnq_e=lnK_F+n^{-1}\ lnC_e$	ln q_e vs. ln C_e		k_F (mg/g(Lmg)$^{1/n}$)	n	r^2
			RB5	51.76	2.95	0.8904
			RR120	45.16	2.8	0.9333
Langmuir	$q_e=(C_e/q_0)+(1/k_Lq_0)$	(C_e/q_e) vs. C_e		q_0 (mg/g)	k_L (L/mg)	r^2
			RB5	175.4	0.265	0.9987
			RR120	172.41	0.202	0.9993
Temkin	$q_e=B\ln K_T+B\ln C_e$	q_e vs. lnC_e		B	K_T (L/mg)	r^2
			RB5	33.59	3.54	0.9677
			RR120	34.26	2.47	0.9895

curve (q_t vs. $t^{0.5}$) has multi-linearity, it implies that two or more controlling steps affect the adsorption process [34]. The effect of contact time on the removal efficiency of dyes by PAC-MNPs was evaluated under the optimized conditions for a time period of 60 min. As shown in Fig. 4, the rate of dye adsorption onto PAC-MNPs was initially fast, then decreased gradually until the equilibrium was reached to a point beyond which no further adsorption could be observed. The rapid increase of the ad- sorption capacity, in the initial stages, could be due to the existence of enormous vacant active sites on the adsorbent surface. Herein, the equilibrium state of RB5 and RR120 adsorption onto PAC-MNPs was met around 40 min contact time.

The validity of studied models was checked by applying the correlation coefficient (r^2). The high correlation coefficient of the pseudo-second-order model, compared with the other models, implies that the pseudo-second-order is the best fit for the experimental data. Furthermore, the calculated amount of q_e, derived from the pseudo-first order model, is not coherent with the experimental data. However, good agreement was obtained when q_e was calculated according to pseudo-second-order model. The plots of kinetic adsorption (see Fig. 4 (insert)) also suggest that the experimental data of RB5 and RR120 adsorption onto the PAC-MNPs are in agreement with pseudo-second order model. This finding indicates that the adsorption of both dyes is controlled via chemisorption [37,46]. Chemisorption consists of sharing or exchanging the electrons between the molecules of dyed and the binding sites of PAC-MNPs, which is reported by Konicki et al. (year) [41]. As shown in Table 5, the value of C_i>0 indicates that intra-particle diffusion is not the only controlling step for the adsorption of both dyes; but also, the process is controlled to some degrees by boundary layer diffusion.

The adsorption isotherm is of great importance in designing a typical adsorption system. The equations of the equilibrium isotherm models were applied to describe the adsorption of RB5 and RR120 dyes in the range of 50 to 200 mg/L onto the PAC-MNPs with the adsorbent dosage and temperature of 1 g/L and 25±1 °C, respectively. Langmuir, Freundlich and Temkin models were also used for modeling the adsorption process of dyes. The equations and parameters of applied equilibrium models for the adsorption process are listed in Table 5. In this table, q_o (mg/g) is maximum adsorbent-phase concentration of the adsorbate when the surface site is saturated with it and k_L (L mg^{-1}) is Langmuir adsorption constant. k_F (mg/g(Lmg)$^{1/n}$) and n are the adsorption capacity and the adsorption intensity, respectively. K_T is the binding constant

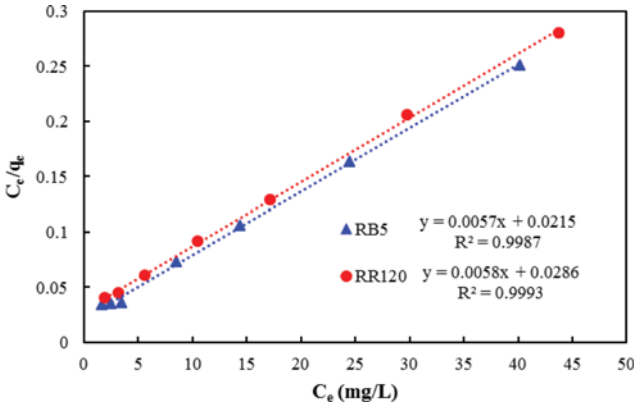

Fig. 5. Plots of Langmuir isotherm of RB5 an RR120 dyes adsorption on PAC-MNPs (experimental conditions: C_0=50-200 mg/L, adsorbent dose=1 g/L, pH 4±0.5, contact time=40 min and 25±1 °C).

representing the maximum binding energy (L/mg) and B (B=RT/b) is the Temkin constant, which depends on temperature. Additionally, R and b stand for the universal gas constant (8.314 J/mol K) and the Temkin constant, respectively. The latter constant is related to the heat of the adsorption and T is the absolute temperature in Kelvin.

As shown in Table 5, the Langmuir isotherm model provides better fitting with experimental data regarding the r^2 value, in comparison with the other models. Generally, the adsorption isotherm models fitted the data in accordance to the following order: Langmuir>Freundlich>Temkin. The values of Freundlich adsorption heterogeneity factor (n) were in the range of 2 to 10, indicating that RB5 and RR120 dyes were favorably adsorbed by PAC-MNPs [12]. As shown in Fig. 5, there is a significant correspondence between experimental data and Langmuir isotherm model. This also confirms that the adsorption process occurs on a homogeneous surface, so the adsorption of RB5 and RR120 dyes on PAC-MNPs occurs in a monolayer manner. Similar observations have been reported in previous studies [47-50].

The maximum adsorption capacities based on the Langmuir model for RB5 and RR120 dyes were 175.4 and 172.4 mg/g, respectively. Table 6 shows a comparison between the obtained values of q_m with several other adsorbents reported in the literature. The q_m values of PAC-MNPs for RB5 and RR120 are higher than that of the majority of other adsorbents, demonstrating that the PAC-

Table 6. Comparison of maximum adsorption capacity of different adsorbents for RB5 and RR120 removal from aqueous media

Adsorbent	Maximum adsorption capacity (mg/g)		Reference
	RB5	RR120	
Modified basic oxygen furnace slag	60	55	[47]
Cotton plant wastes-stalk	35.7	-	[51]
Peanut hull	55.5		[45]
Fe_3O_4 nanoparticles	-	166.7	[52]
Modified magnetic chitosan microspheres	-	144.9	[53]
Chara contraria	-	112.8	[54]
PAC-MNPs	175.4	172.4	This study

Table 7. The values of thermodynamic parameters for the adsorption of RB5 and RR120 on the PAC-MNPs at various temperatures

Dye	T (°C)	Parameters			
		ln K	ΔG^o (kJ/mol)	ΔH^o (kJ/mol)	ΔS^o (kJ/mol·K)
RB5	25	3.6	−8.92	22.17	0.125
	35	3.72	−9.52		
	45	4.04	−10.68		
RR120	25	3.27	−8.1	20.67	0.087
	35	3.65	−9.34		
	45	3.98	−10.52		

MNPs can be considered as one of the most effective adsorbents for RB5 and RR120 adsorption.

The thermodynamic parameters provide a deeper mechanistic understanding of the adsorption process. In this study, thermodynamic parameters of reactive dyes adsorption on the PAC-MNPs were determined at various temperatures ranging from 25 to 45 °C with 50 mg/L of dyes and 1 g/L of the adsorbent; the results are shown in Table 7. The thermodynamic parameters of the adsorption process comprise standard enthalpy (ΔH^o), standard entropy (ΔS^o) and free energy change (ΔG^o). Van't Hoff equation shown in Eq. (8) indicates a relationship between the temperature (T) and equilibrium constant of the adsorption ($K=q_e/C_e$). The values of ΔH^o and ΔS^o were obtained from the slope and intercept of the plot of $\ln q_e/C_e$ versus 1/T, respectively.

$$\ln\left(\frac{q_e}{C_e}\right)=\frac{\Delta S^o}{R}-\frac{\Delta H^o}{RT} \quad (8)$$

where, q_e is the amount of adsorbed dye at equilibrium state (mg/g) and C_e is the equilibrium concentration of dye in the solution (mg/L). The values of ΔG^o can be calculated from the Gibbs free energy equation, which is shown below:

$$\Delta G^o=-RT\ln K \quad (9)$$

In this study, as shown in Table 7, positive values were obtained for ΔH^o and ΔS^o. The positive value of ΔH^o implies that the adsorption process of the reactive dyes was endothermic. In addition, the obtained positive values of ΔS^o confirm the affinity of the PAC-MNPs towards RB5 and RR120 dyes [34]. However, the negative values o btained for the ΔG^o demonstrate that the adsorption of both dyes on PAC-MNPs occurs spontaneously and is feasible [55,56].

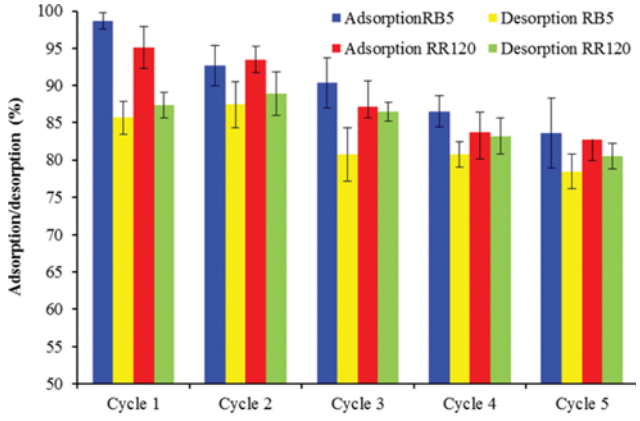

Fig. 6. RB5 and RR120 dyes adsorption on the PAC-MNPs adsorbent with five adsorption–regeneration cycles.

7. Desorption, Reusability and Stability of PAC-MNPs

As shown in Fig. 6, the adsorption percentages of RB5 and RR120 dyes by PAC-MNPs were not statistically significant. It is noteworthy that the adsorption percentage started decreasing trend after five cycles. This confirms that the PAC-MNPs can be recycled and reused for at least five successive cycles without any significant loss in the efficiency of the adsorption process. The slight loss of efficiency could be due to the filling some active sites by dye molecules causing a reduction in the specific surface area of the adsorbent, which consequently reduces the adsorption capacity of the adsorbent. It was also found that more than 78.44% and 80.5% of the adsorbed RB5 and RR120, respectively, could be desorbed and recovered from the adsorbent surface in the fifth cycle and in the presence of NaOH. Generally, these results ensured that the PAC-MNPs can be applied as a cost-effective and efficient adsorbent for the treatment of textile wastewaters. In fact, the proposed adsorbent in this study shows a good potential of regeneration and reusability, which are both of high importance in industrial applications.

To evaluate the stability of the PAC-MNPs composite, the concentrations of dissolved iron ions in the solution during the five consecutive cycles were measured. The concentration of dissolved iron in the reaction solution in all studied cycles was measured (<0.2 mg/L) to be compared with the maximum acceptable concentration level in drinking water (0.3 mg/L) set by the WHO [57]. It suggests that the MNPs species were strongly embedded into mesoporous matrix of the PAC through stable bonding. This also ensures that iron leaching from PAC-MNPs surface might not result in metal pollution in water. Therefore, it can be concluded that PAC-MNPs composite has a good stability and can be used as a promising adsorbent for removing dyes from the aquatic environment with negligible loss of magnetic properties, even under acidic conditions.

8. Wastewater Treatment

The potential application of PAC-MNPs for removing reactive dyes from wastewater was tested by determining the composite adsorption efficiency using a dye-industry wastewater sample contained a series of dyes. The concentration of RB5 and RR120 dyes in wastewater was set in the range of 10-40 mg/L. The pH of samples was adjusted to 4.0±0.2, and then 1 g/L of PAC-MNPs was added to each solution. After equilibrating for 40 min, the adsorbent was separated, and the concentrations of RB5 and RR120 were determined. The percentages of dye removal by the PAC-MNPs in the DI-water and wastewater containing 10-40 mg/L concentrations of RB5 and RR120 are shown in Fig. 7. As can be seen, PAC-MNPs almost completely removed 10 and 20 mg/L concentrations of dyes in both the DI-water and real environments. Generally, the removal percentages in the wastewater samples were slightly lower, compared to the DI-water samples. Thus, the pres-

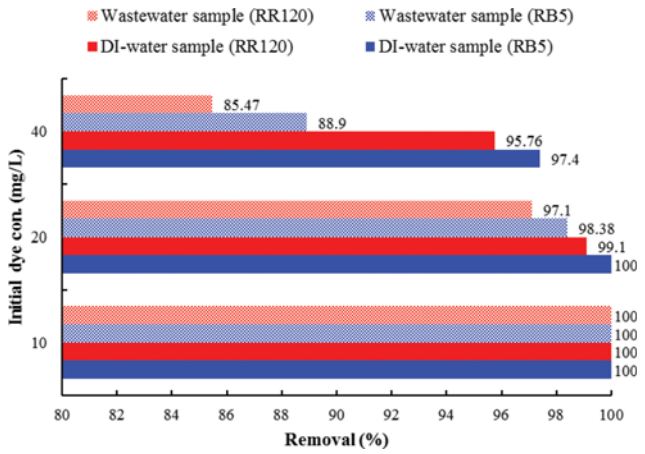

Fig. 7. Removal percentage of RB5 and RR120 dyes by PAC-MNPs in DI-water and wastewater samples (experimental conditions: C_0=10-40 mg/L, adsorbent dose=1 g/L, pH 4±0.5, contact time=60 min and 25±1 °C).

ence of solid and interfering ions can lead to a slight reduction in the adsorption efficiency. Based on the obtained results, it can be implied that the PAC-MNPs have a good anti-interference potential for the removal of reactive dyes in dye-industry wastewaters. Hence, it can be postulated that the removal of RB5 and RR120 dyes from industrial wastewaters using the PAC-MNPs as a magnetic adsorbent can be a cost-effective and useful process.

CONCLUSION

PAC was modified with magnetite nanoparticles to prepare an adsorbent (PAC-MNPs) for reactive dyes (RB5 and RR120) adsorption from aqueous solution in a batch system. Based on the obtained results, an increase in the temperature, contact time and the adsorbent dosage and a decrease in the initial dye concentration resulted in the improvement of the adsorption efficiency. The studies of the adsorption isotherm and kinetic models showed that the adsorption of both dyes onto PAC-MNPs can be modeled using Langmuir isotherm and pseudo-second order kinetic models. In addition, the findings showed high adsorption capacity, easy and simple separation and good regeneration and reusability for PAC-MNPs, which make it an optimal and efficient adsorbent in removing dye from the aquatic environments. According to our findings, it can be implied that the magnetization of adsorbents and the use of magnetic separation techniques are the effective approaches in resolving problems associated with centrifuge and filtration.

CONFLICT OF INTEREST

The authors have declared no conflict of interest.

ACKNOWLEDGEMENTS

The present work was financially supported by the Student Research Committee Ahvaz Jundishapur University of Medical Sciences under grant no. 95S.31.

SUPPORTING INFORMATION

Additional information as noted in the text. This information is available via the Internet at http://www.springer.com/chemistry/journal/11814.

REFERENCES

1. A. A. Babaei, A. Khataee, E. Ahmadpour, M. Sheydaei, B. Kakavandi and Z. Alaee, *Korean J. Chem. Eng.*, **33**, 1352 (2015).
2. V. K. Gupta, R. Jain, A. Mittal, T. A. Saleh, A. Nayak, S. Agarwal and S. Sikarwar, *Mater. Sci. Eng.: C.*, **32**, 12 (2012).
3. A. Mittal, J. Mittal, A. Malviya and V. K. Gupta, *J. Colloid Interface Sci.*, **340**, 16 (2009).
4. R. Rezaei Kalantry, A. Jonidi Jafari, A. Esrafili, B. Kakavandi, A. Gholizadeh and A. Azari, *Desalination and Water Treatment.*, **57**, 6411 (2016).
5. A. Mittal, J. Mittal, A. Malviya, D. Kaur and V. K. Gupta, *J. Colloid Interface Sci.*, **342**, 518 (2010).
6. M. Rafatullah, O. Sulaiman, R. Hashim and A. Ahmad, *J. Hazard. Mater.*, **177**, 70 (2010).
7. Y. Yao, L. Wang, L. Sun, S. Zhu, Z. Huang, Y. Mao, W. Lu and W. Chen, *Chem. Eng. Sci.*, **101**, 424 (2013).
8. M. A. Ahmad and R. Alrozi, *Chem. Eng. J.*, **171**, 510 (2011).
9. M. Ghaedi, B. Sadeghian, A. A. Pebdani, R. Sahraei, A. Daneshfar and C. Duran, *Chem. Eng. J.*, **187**, 133 (2012).
10. V. K. Gupta, R. Jain, A. Nayak, S. Agarwal and M. Shrivastava, *Mater. Sci. Eng.: C.*, **31**, 1062 (2011).
11. N. Jaafarzadeh, B. Kakavandi, A. Takdastan, R. R. Kalantary, M. Azizi and S. Jorfi, *RSC Adv.*, **5**, 84718 (2015).
12. A. Azari, B. Kakavandi, R. R. Kalantary, E. Ahmadi, M. Gholami, Z. Torkshavand and M. Azizi, *J. Porous Mater.*, **22**, 1083 (2015).
13. A. R. Esfahani, S. Hojati, A. Azimi, M. Farzadian and A. Khataee, *J. Taiw. Inst. Chem. Eng.*, **49**, 172 (2014).
14. V. K. Gupta, I. Ali, T. A. Saleh, M. Siddiqui and S. Agarwal, *Environ. Sci. Pollut. Res.*, **20**, 1261 (2013).
15. V. K. Gupta, Suhas, *J. Environ. Manage.*, **90**, 2323 (2009).
16. T. A. Saleh and V. K. Gupta, *Adv. Colloid Interface Sci.*, **211**, 93 (2014).
17. T. A. Saleh and V. K. Gupta, *Environ. Sci. Pollut. Res.*, **19**, 1224 (2012).
18. A. A. Babaei, M. Bahrami, A. Farrokhian Firouzi, A. Ramazanpour Esfahani and L. Alidokht, *Desalination and Water Treatment.*, **56**, 3380 (2015).
19. B. Kakavandi, A. Jonidi Jafari, R. Rezaei Kalantary, S. Nasseri, A. Esrafili, A. Gholizadeh and A. Azari, *J. Chem. Technol. Biotechnol.*, (2016), DOI:10.1002/jctb.4925.
20. B. Kakavandi, A. Takdastan, N. Jaafarzadeh, M. Azizi, A. Mirzaei and A. Azari, *J. Photochem. Photobiol. A: Chem.*, **314**, 178 (2016).
21. V. K. Gupta, S. K. Srivastava, D. Mohan and S. Sharma, *Waste Manage.*, **17**, 517 (1998).
22. V. K. Gupta and A. Nayak, *Chem. Eng. J.*, **180**, 81 (2012).
23. J. Yang, Y. Dong, J. Li, Z. Liu, F. Min and Y. Li, *Korean J. Chem. Eng.*, **32**, 2247 (2015).
24. B. Kakavandi, R. R. Kalantary, A. J. Jafari, S. Nasseri, A. Ameri, A. Esrafili and A. Azari, *CLEAN - Soil, Air, Water*, **43**, 1157 (2015).
25. A. Afshar, S. A. S. Sadjadi, A. Mollahosseini and M. R. Eskandar-

ian, *Korean J. Chem. Eng.*, **33**, 669 (2016).
26. J.-L. Gong, B. Wang, G.-M. Zeng, C.-P. Yang, C.-G. Niu, Q.-Y. Niu, W.-J. Zhou and Y. Liang, *J. Hazard. Mater.*, **164**, 1517 (2009).
27. V. K. Gupta, R. Kumar, A. Nayak, T. A. Saleh and M. A. Barakat, *Adv. Colloid Interface Sci.*, **193-194**, 24 (2013).
28. H.-Y. Zhu, R. Jiang, L. Xiao and W. Li, *J. Hazard. Mater.*, **179**, 251 (2010).
29. J. Huang, Z. Wu, L. Chen and Y. Sun, *J. Mol. Liq.*, **209**, 753 (2015).
30. American Society for Testing and Material (ASTM) (2012).
31. Y. Tang, S. Liang, S. Yu, N. Gao, J. Zhang, H. Guo and Y. Wang, *Colloids Surf., A: Physicochem. Eng. Aspects.*, **406**, 61 (2012).
32. Ş. S. Bayazit and Ö. Kerkez, *Chem. Eng. Res. Design*, **92**, 2725 (2014).
33. K. P. Singh, S. Gupta, A. K. Singh and S. Sinha, *J. Hazard. Mater.*, **186**, 1462 (2011).
34. A. Mohseni-Bandpi, B. Kakavandi, R. R. Kalantary, A. Azari and A. Keramati, *RSC Adv.*, **5**, 73279 (2015).
35. S. Nethaji, A. Sivasamy and A. B. Mandal, *Bioresour. Technol.*, **134**, 94 (2013).
36. T. Depci, *Chem. Eng. J.*, **181**, 467 (2012).
37. B. Kakavandi, M. Jahangiri-rad, M. Rafiee, A. R. Efahani and A. A. Babaei, *Micropor. Mesopor. Mater.*, **231**, 192 (2016).
38. M. H. Muhamad, S. R. Sheikh Abdullah, A. B. Mohamad, R. Abdul Rahman and A. A. Hasan Kadhum, *J. Environ. Manage.*, **121**, 179 (2013).
39. A. Mittal, D. Kaur, A. Malviya, J. Mittal and V. K. Gupta, *J. Colloid Interface Sci.*, **337**, 345 (2009).
40. A. Mittal, J. Mittal, A. Malviya and V. K. Gupta, *J. Colloid Interface Sci.*, **344**, 497 (2010).
41. W. Konicki, I. Pełech, E. Mijowska and I. Jasińska, *CLEAN-Soil Air Water.*, **42**, 284 (2014).
42. A. R. Esfahani, A. F. Firouzi, G. Sayyad, A. Kiasat, L. Alidokht and A. Khataee, *Research on Chemical Intermediates*, **40**, 431 (2014).
43. A. R. Esfahani, S. Hojati, A. Azimi, L. Alidokht, A. Khataee and M. Farzadian, *Korean J. Chem. Eng.*, **31**(4), 630 (2014).
44. A. H. Sulaymon and W. M. Abood, *Desalination and Water Treatment.*, **52**, 5485 (2014).
45. M. Ş. Tanyildizi, *Chem. Eng. J.*, **168**, 1234 (2011).
46. V. K. Gupta, A. Nayak and S. Agarwal, *Environ. Eng. Res.*, **20**, 1 (2015).
47. Y. Xue, H. Hou and S. Zhu, *Chem. Eng. J.*, **147**, 272 (2009).
48. K. Z. Elwakeel and M. Rekaby, *J. Hazard. Mater.*, **188**, 10 (2011).
49. A. Jain, V. Gupta and A. Bhatnagar, Suhas, *Sep. Sci. Technol.*, **38**, 463 (2003).
50. M. Massoudinejad, A. Asadi, M. Vosoughi, M. Gholami, B. Kakavandi and M. Karami, *Korean J. Chem. Eng.*, **32**, 2078 (2015).
51. Ö. Tunc, H. Tanacı and Z. Aksu, *J. Hazard. Mater.*, **163**, 187 (2009).
52. G. Absalan, M. Asadi, S. Kamran, L. Sheikhian and D. M. Goltz, *J. Hazard. Mater.*, **192**, 476 (2011).
53. Z. Li, M. Cao, W. Zhang, L. Liu, J. Wang, W. Ge, Y. Yuan, T. Yue, R. Li and W. W. Yu, *Food Chem.*, **145**, 749 (2014).
54. A. Celeklia, G. İlgün and H. Bozkurt, *Chem. Eng. J.*, **191**, 228 (2012).
55. A. Azari, R. R. Kalantary, G. Ghanizadeh, B. Kakavandi, M. Farzadkia and E. Ahmadi, *RSC Adv.*, **5**, 87377 (2015).
56. V. K. Gupta, S. Agarwal and T. A. Saleh, *J. Hazard. Mater.*, **185**, 17 (2011).
57. W. H. Organization, Guidelines for drinking-water quality: First addendum to volume 1, Recommendations, World Health Organization (2006).

Supporting Information

Application of mesoporous magnetic carbon composite for reactive dyes removal: Process optimization using response surface methodology

Ahmad Jonidi Jafari[*,], Babak Kakavandi[***,****,†], Roshanak Rezaei Kalantary[*,**], Hamed Gharibi[*****], Anvar Asadi[******], Ali Azari[*******], Ali Akbar Babaei[****], and Afshin Takdastan[****]**

*Research Center for Environmental Health Technology (RCEHT), Iran University of Medical Sciences, Tehran, Iran
**Department of Environmental Health Engineering, School of Public Health, Iran University of Medical Sciences, Tehran, Iran
***Student Research Committee, Ahvaz Jundishapur University of Medical Sciences, Ahvaz, Iran
****Department of Environmental Health Engineering, School of Health, Ahvaz Jundishapur University of Medical Sciences, Ahvaz, Iran
*****School of Public Health, Shahroud University of Medical Sciences, Shahroud, Iran
******Department of Environmental Health Engineering, School of Public Health, Shahid Beheshti University of Medical Sciences, Tehran, Iran
*******Department of Environmental Health Engineering, School of Public Health, Tehran University of Medical Sciences, Tehran, Iran
(*Received 17 February 2016 • accepted 8 June 2016*)

Table S1. The structure and some of the important physicochemical properties of RB5 and RR120 dyes

Characteristic	Dye	
	RB5	RR120
Chemical formula	$C_{26}H_{21}N_5Na_4O_{19}S_6$	$C_{44}H_{24}Cl_2N_{14}Na_6O_{20}S_6$
Commercial name	Reactive Black 5	Reactive Red 120
Abbreviation	RB5	RR120
Class	Di-azo	Di-azo
C.I. number	20,505	292775
Molecular weight (g/mol)	991.82	1469.98
λ_{max} (nm)	597	515
Molecular structure	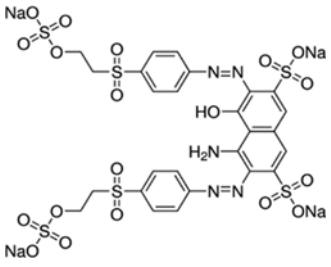	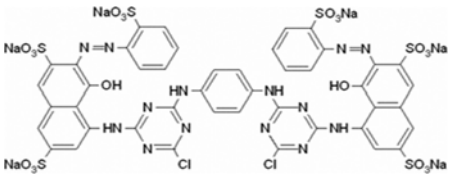

Table S2. Analysis of variance (ANOVA) for response surface quadratic model for RB5 and RR120 dyes removal by the AC-Fe_3O_4

Source	Sum of squares	df	Mean square	F-value	p-Value Prob>F
RB5 dye removal (%)					
Model	4083.23	14	291.66	296.27	<0.0001[s]
X_1- Temperature	139.61	1	139.61	141.82	<0.0001[s]
X_2- Contact time	51.93	1	51.93	52.75	<0.0001[s]
X_3- Adsorbent dose	231.76	1	231.76	235.43	<0.0001[s]
X_4- Initial concentration	473.32	1	473.32	480.81	<0.0001[s]
X_1X_2	44.35	1	44.35	45.05	<0.0001[s]
X_1X_3	12.30	1	12.30	12.49	0.0033[s]
X_1X_4	42.38	1	42.38	43.05	<0.0001[s]
X_2X_3	11.77	1	11.77	11.96	0.0038[s]
X_2X_4	10.47	1	10.47	10.63	0.0057[s]
X_3X_4	59.37	1	59.37	60.31	<0.0001[s]
X_1^2	108.84	1	108.84	110.57	<0.0001[s]
X_2^2	144.71	1	144.71	147.00	<0.0001[s]
X_3^2	208.97	1	208.97	212.28	<0.0001[s]
X_4^2	202.90	1	202.90	206.11	<0.0001[s]
Residual	13.78	14	0.98		
Lack of fit	12.60	10	1.26	4.27	0.0873[ns]
Pure error	1.18	4	0.30		
Cor total	4097.01	28			
R^2=0.9966, adjusted-R^2=0.9933, predicted-R^2=0.9844, Adeq precision=59.42, C. V.%=1.17					
RR120 dye removal (%)					
Model	3700.29	14	264.31	51.27	<0.0001[s]
X_1	30.53	1	30.53	5.92	0.0289[s]
X_2	93.29	1	93.29	18.10	0.0008[s]
X_3	129.13	1	129.13	25.05	0.0002[s]
X_4	740.18	1	740.18	143.57	<0.0001[s]
X_1X_2	3.40	1	3.40	0.66	0.4301[ns]
X_1X_3	0.94	1	0.94	0.18	0.6765[ns]
X_1X_4	23.52	1	23.52	4.56	0.0508[ns]
X_2X_3	0.12	1	0.12	0.023	0.8826[ns]
X_2X_4	3.15	1	3.15	0.61	0.4474[ns]
X_3X_4	39.38	1	39.38	7.64	0.0152[s]
X_1^2	78.69	1	78.69	15.26	0.0016[s]
X_2^2	149.32	1	149.32	28.96	<0.0001[s]
X_3^2	66.10	1	66.10	12.82	0.0030[s]
X_4^2	194.01	1	194.01	37.63	<0.0001[s]
Residual	72.18	14	5.16		
Lack of fit	65.94	10	6.59	4.23	0.0885[ns]
Pure error	6.23	4	1.56		
Cor total	3772.46	28			
R^2=0.9809, adjusted-R^2=0.9617, predicted-R^2=0.8909, Adeq precision=26.02, C. V.%=2.87					

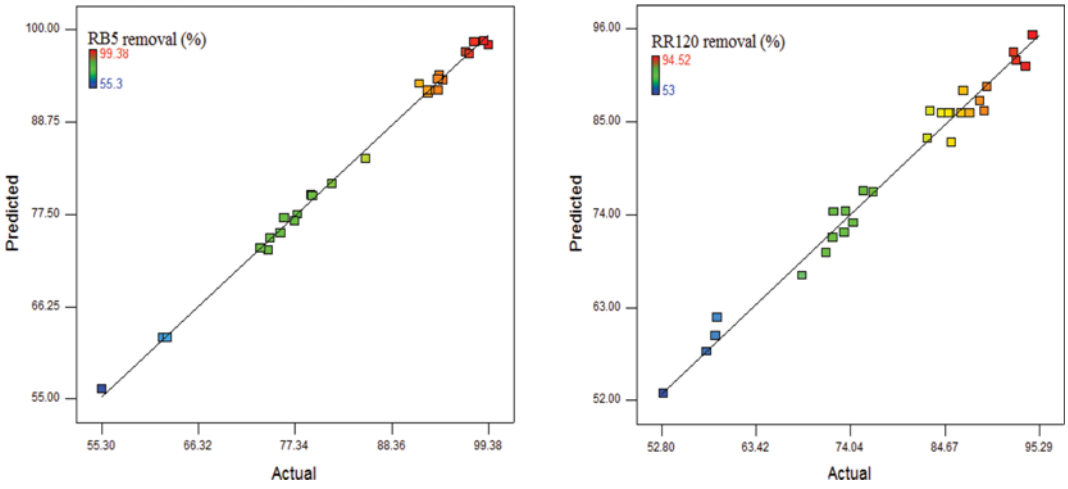

Fig. S1. The actual and predicted response plot of RB5 and RR120 adsorption.

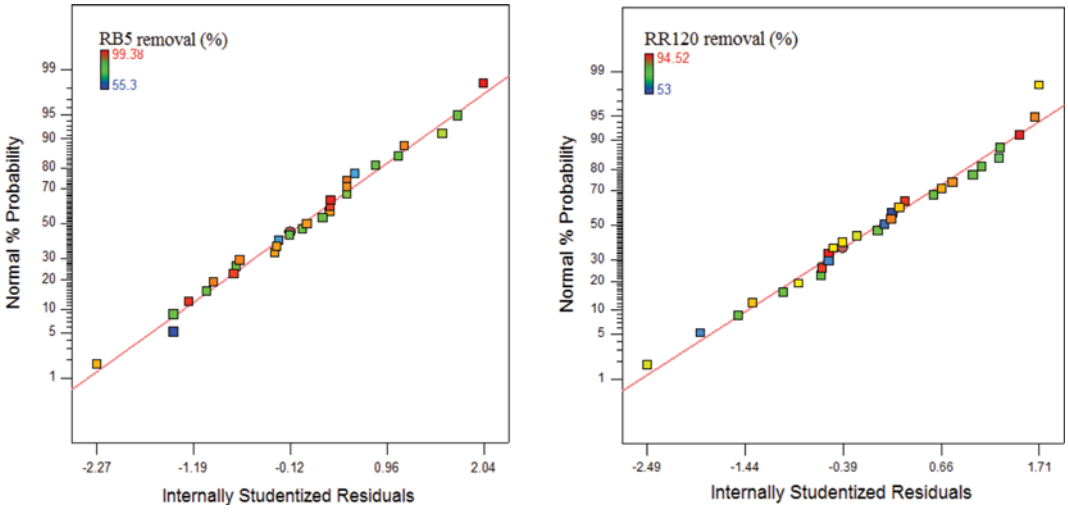

Fig. S2. Normal probability plots of residuals for RB5and RR120 removal.